

Zeolite Mineralization in Mudstones of the East Pauzhetka Thermal Field As an Indicator of the Discharge of Alkaline Fluids in a Present-Day Hydrothermal System, Southern Kamchatka

E. I. Sandimirova^{a, *}, S. N. Rychagov^{a, **}, A. V. Sergeeva^a, and V. M. Chubarov^a

^a Institute of Volcanology and Seismology, Far East Branch, Russian Academy of Sciences,
bulvar Piipa, 9, Petropavlovsk-Kamchatsky, 683006 Russia

*e-mail: sand@kscnet.ru

**e-mail: rychn@kscnet.ru

Received December 6, 2021; revised January 31, 2022; accepted August 23, 2022

Abstract—The argillized deposits of the East Pauzhetka thermal field in the Pauzhetka hydrothermal system were found to contain a zone of intensive zeolitization which consists of medium to high silica calcium zeolite varieties, namely, laumontite, mordenite, heulandite-Ca, and stilbite-Ca. Of all these, stilbite-Ca has the highest abundance. The zeolites can be identified well enough based both on the relationship between Si and Al, which are part of the zeolite framework, and on the concentrations of non-framework cations (Ca, Mg, Na, K, Sr, and Ba). Zeolites are mostly formed in the lower horizons of hydrothermal clays and in the underlying argillized andesites, as deep alkaline chloride-sodium hydrothermal fluids are discharged and are mixed with condensates of acid (up to neutral) vapor. The resulting sequence of zeolite generation in the shallow zone where alkaline solutions are discharged reflects, to a certain degree, a change of zeolite facies in the deeper horizons of the system: from medium-silica laumontite to high silica stilbite-Ca. We have thereby a general inference as to the regressive directivity of hydrothermal metamorphic processes in the Pauzhetka system structure, from medium-temperature propylites generated during the paleo phase to the present-day low-temperature mudstones.

Keywords: hydrothermal system, mudstones, discharge of alkaline hydrothermal fluids, medium- and high-silica zeolites

DOI: 10.1134/S0742046322060070

INTRODUCTION

Zeolites (the word was coined by combining two Greek words meaning *to boil* and *stone*) are hydrated aluminosilicates of alkaline and alkaline-earth metals with an open hollow-framework structure (Betekhtin, 1950; Senderov and Khitarov, 1970; Fersman, 1952; Barth-Wirching and Holler, 1989; Passaglia and Shepard, 2001; Smith et al., 1963). At present we know over 80 mineral species of naturally occurring zeolites (Godovikov, 1975; Distanov et al., 1990; Lazarenko, 1971; *The Encyclopedia of Mineralogy*, 1981; Chelishchev, 1980; Coombs et al., 1997; Gottardi, 1989; Marantos et al., 2011). These minerals were not specially noticed until the mid-20th century. However, when their remarkable physical and chemical properties (ion-exchange, adsorption, catalytic properties among others) had been discovered, and they began to be used in practice, an enormous number of publications were devoted to zeolites during recent decades (Kossovskaya, 1975; Pekov et al., 2004; Suprychev, 1978, 1980; Chelishchev et al., 1987; Aoki, 1978;

Boles, 1977; Mumpton, 1999; Ortiz et al., 2011; Sheppard, 1973, among others).

Zeolites widely occur in platforms, in oceanic and lacustrine sediments, in volcanic rocks, in soils, and in other environments. They are generated by hypergenesis, epigenesis, diagenesis, regional metamorphism, late magmatic and hydrothermal-metasomatic processes (Kossovskaya et al., 1980; *Prirodnye tseolity*, 1980; Senderov and Khitarov, 1970; Suprychev and Kirikilitza, 1980; Jijima and Utada, 1972; Sheppard and Gude, 1973; Zozulya et al., 2018). The most significant storage of zeolites and the greatest diversity in their mineral species occur in volcanogenic and volcano-sedimentary rocks that have been affected by hydrothermal metasomatic alteration (Naboko and Glavatskikh, 1978; Nasedkin et al., 1988; Petrova, 2005; Suprychev, 1978; Shevchuk, 2008; Coombs et al., 1959). Zeolitization in areas of recent and Quaternary volcanism occurs at relatively low temperatures and pressures in zones where hydrothermal systems are being discharged, consequently associates with argillization (Naboko, 1980; Rochler, 1972;

Moncure et al., 1981). One typical example of simultaneous zeolitization and argillization is the Pauzhetka hydrothermal system (HS) (Naboko, 1963; *Pauzhetkie ...*, 1965; *Struktura ...*, 1993).

Zeolite generation in the Pauzhetka HS structure occurs widely, both over the area and down to the bottom of the section so far studied (800–1000 m) (Korobov et al., 1992; Naboko, 1963; Pampura, 1977, 1980; *Struktura ...*, 1993), while the Pauzhetka geothermal field is viewed as having potential for raw zeolite, with its predicted reserves being evaluated as 200 million tons (Burov et al., 1992; Naboko, 1980). S.I. Naboko, and subsequently A.D. Korobov, identified two phases of zeolite generation, the paleo phase (apparently Pleistocene to Lower Holocene) and the present-day phase (Korobov, 2019; Naboko et al., 1965). Zeolitization occurred in all types of rock during the earlier phase. The most vigorous zeolitization occurred in the upper HS horizons, in tuffs of the Lower and Middle Pauzhetka subformations, which were the more permeable to heat flux; they formed thick (reaching depths of a few hundreds of meters) zeolitization zones (*Struktura ...*, 1993). The present-day mineralization is thought to include the zeolite mineralization superposed upon the earlier zeolitized rocks of the section; this type of mineralization is seen as monomineral and more complex veinlets, cavity and pore fillings, as well as being observed in sediments left by thermal springs, in pipelines and other technical facilities, including the mineralization obtained in experimental research where minerals are grown in geothermal boreholes (Eroshchev-Shak, 1992; Karpov, 1976; Lebedev, 1979; Naboko and Lebedev, 1964; Naboko et al., 1965).

The present-day zeolite generation in the Pauzhetka HS is little known. A study of mineral associations within thermal fields using advanced surveying methods has revealed new aspects in the generation of zeolite minerals. As an example, we have identified, at the bottom of the hydrothermal clay sequence in the East Pauzhetka thermal field, a carbonatization–zeolitization zone of argillized andesites that shows uncommon chemical and mineral compositions; that zone includes recently formed sulfides, titanium- and zircon-silicates, phosphates of calcium and of rare metals (Rychagov et al., 2017), as well as obtaining first characteristics of the zeolite sampled in that zone (Rychagov et al., 2018). Subsequent studies showed that the section of the East Pauzhetka thermal field contains different species of zeolites in a very narrow depth interval, while their distribution obeys a vertical metasomatic zonality (Sandimirova et al., 2021).

The present publication describes the results of a study of zeolite mineralization in argillized rocks sampled in the East Pauzhetka thermal field of the Pauzhetka HS. We characterize the morphology and internal structure of zeolite minerals, their chemical and species composition, individual features of each mineral

species, and the distribution of zeolites in the section of the thermal field, as well as evaluating the physicochemical conditions of their generation.

GENERAL INFORMATION ON THE ZEOLITES THAT WERE PREVIOUSLY DIAGNOSED IN THE PAUZHETKA HYDROTHERMAL SYSTEM

There is mention in the literature of eleven zeolite species that are encountered in the hydrothermally altered rocks of the Pauzhetka HS: analcime, wairakite, harmotome, heulandite (clinoptilolite), desmine, laumontite (β -leonhardtite), ptilolite, scolecite, thomsonite, phillipsite, and chabasite (Table 1). Of these, the most abundant minerals are analcime, desmine, laumontite, and ptilolite. A few, six zeolite species (wairakite, heulandite, desmine, laumontite, mordenite, and thomsonite), are provided with detailed descriptions of their morphology with indication of optic and X-ray characteristics, as well as having a few analyses of chemical composition (Naboko, 1963, 1980; Naboko et al., 1965; Lebedev, 1979; Korobov, 2019). The names of some minerals are now obsolete. According to the nomenclature approved by the International Zeolite Association, leonhardtite is a low-water laumontite, desmine corresponds to stilbite, ptilolite corresponds to mordenite, while clinoptilolite ($\text{Si}/\text{Al} \geq 4$) and heulandite ($\text{Si}/\text{Al} < 4$) make an isomorphous series and belong to the same species (Coombs et al., 1997; Passaglia and Sheppard, 2001).

A DESCRIPTION OF THE EAST PAUZHETKA THERMAL FIELD

The East Pauzhetka thermal field (EPF) lies in the western slope of the Kambalny volcanic mountain range—a resurgent tectono-magmatic uplift in the Pauzhetka volcano-tectonic depression (*Dolgozhivushchii ...*, 1980). The EPF is, like the other shallow regions where vapor-dominated hydrothermal fluids are discharged in the Pauzhetka HS, confined to a circular uplifted Quaternary block (*Struktura ...*, 1993). The field has overall dimensions of $\geq 250 \times 500$ m, the size of the hottest part is 60×120 m (Fig. 1). The thermal occurrences include steaming soils, vapor-gas jets, mud-water pots, and warm lakes. The maximum temperatures of the thermal waters that are formed at the ground surface by condensation of vapor are 98°C , the temperatures are $105\text{--}107^\circ\text{C}$ in the soils, and $108\text{--}109^\circ\text{C}$ in the vapor-gas jets. The thermal waters are acid sulfate and low-acid hydrocarbonate-sulfate ones with a wide range of cation composition, with the total salinity being below 0.8 g/L.

The soils are hydrothermal clays that make an uninterrupted cover extending far beyond the limits of the current hot area. Figure 2 shows a generalized section of the EPF argillized rocks. The clay sequence has a stratified structure (Rychagov et al., 2017, 2019; Feofilaktov et al., 2017). The upper horizon is a typical

Table 1. Naturally occurring zeolites encountered in hydrothermally altered rocks of the Pauzhetka hydrothermal system based on data from the literature

No.	(Naboko, 1963, 1980; Naboko et al., 1965)	(Lebedev, 1979)	(Korobov, 2019)
	Minerals		
1	Analcime		Analcime
2	Wairakite	Wairakite	Wairakite
3	Heulandite	Heulandite	Heulandite (clinoptilolite)
4	Harmotome		
5	Desmine = stilbite*	Desmine (stellerite)** = = stilbite*	
6	Laumontite	Laumontite	Laumontite β-leonhardite = laumontite*
7	Ptilolite = mordenite*	Mordenite	Mordenite
8	Scolecite		
9	Thomsonite	Thomsonite	
10	Phillipsite		
11	Chabasite		

* Mineral names follow the classification adopted by the International Zeolite Association, IZA (Coombs et al., 1997). **Stellerite is treated as a purely calcium variety of desmine (Lebedev, 1979).

zone of sulfuric acid leaching. The clays are composed of kaolinite, hydroxides, and oxides of Fe and Ti; of sulfates of Fe, Ca, and other metals; of opal; and of chalcedony. Some patches retain the pseudomorphous structure of blocky jointing that was retained from the original rocks, namely, andesitic lavas. The horizon has a thickness that varies between 50–80 cm in the middle of the hot patch and >300–350 cm at its periphery. The section below contains a horizon 150 cm thick on average composed of plastic montmorillonite clays. It typically contains numerous lenses, films, and thin veinlets of opal, α-quartz, and pyrite dispersed throughout the groundmass. The horizon and the underlying clays saturated with sulfides (up to 20 vol % or greater) can be classified as “blue clays” (Rychagov et al., 2009). As has been mentioned above, the plastic clay horizon is an aquifuge and a thermal screen, which controls the generation of diverse mineral associations in the EPF structure (Rychagov et al., 2017). Under this horizon there are two zones (from bottom to top) that are distinguishable in some sections: a silica–carbonate–sulfide zone and a phosphate–alumosilicate–sulfide one. Toward the western boundary of the field, the two zones are combined in a single one that has a more complex structure. The underlying horizon of “dry” sulfidized clays has also a persistent attitude along the strike of the thermal field. The deposits at the location consist of smectite clay with abundant dispersed coarse-crystalline (up to 2–3 mm) pyrite and semi-decomposed andesite clasts. One notes a typical occurrence of fragments (up to 15–25 vol %) saturated with siliceous alumosilicate material: they make interbeds, lenses, and “spots” in the main matrix. It is more likely that the fragments were produced in a metasomatic manner by replacing

andesite clasts with siliceous minerals, as well as with smectites etc. At the periphery of the field the horizon is composed of typical “blue clay”, and it is thicker there.

The bottom of the clay sequence consists of metasomatic breccias in andesites and of strongly cracked andesites. The andesites are almost completely altered to become a zeolite–carbonate–chlorite–silica–alumosilicate aggregate that occurs both in the groundmass (in cement and in fragments of breccia “clasts”) and in the cracked pore space (Rychagov et al., 2021). The maximum depth of this section reached by boreholes is 10 m.

THE METHOD OF STUDY

The samples for study were obtained from core holes using a standardized small-size KMB-2-10 machine and proceeding by detailed layer-by-layer core recovery, in intervals of 20 cm of geological section on average.

The morphology, structure, and chemical composition of the zeolites were studied using a VEGA3 scanning electron microscope equipped with an OXFORD analytical instruments X-MAX80 attachment with company-supplied software AZtec (Institute of Volcanology and Seismology (IV&S), Far East Branch (FEB), Russian Academy of Sciences (RAS) Petropavlovsk-Kamchatsky, Analyst V.M. Chubarov, Operator E.I. Sandimirova). Chemical elements were determined by comparing them to a series of standards whose composition was tested for homogeneity and element concentration: sanidine (Si, Na, K), Al₂O₃ (Al); diopside (Ca), MgO (Mg), Fe (Fe), SrSO₄ (Sr),

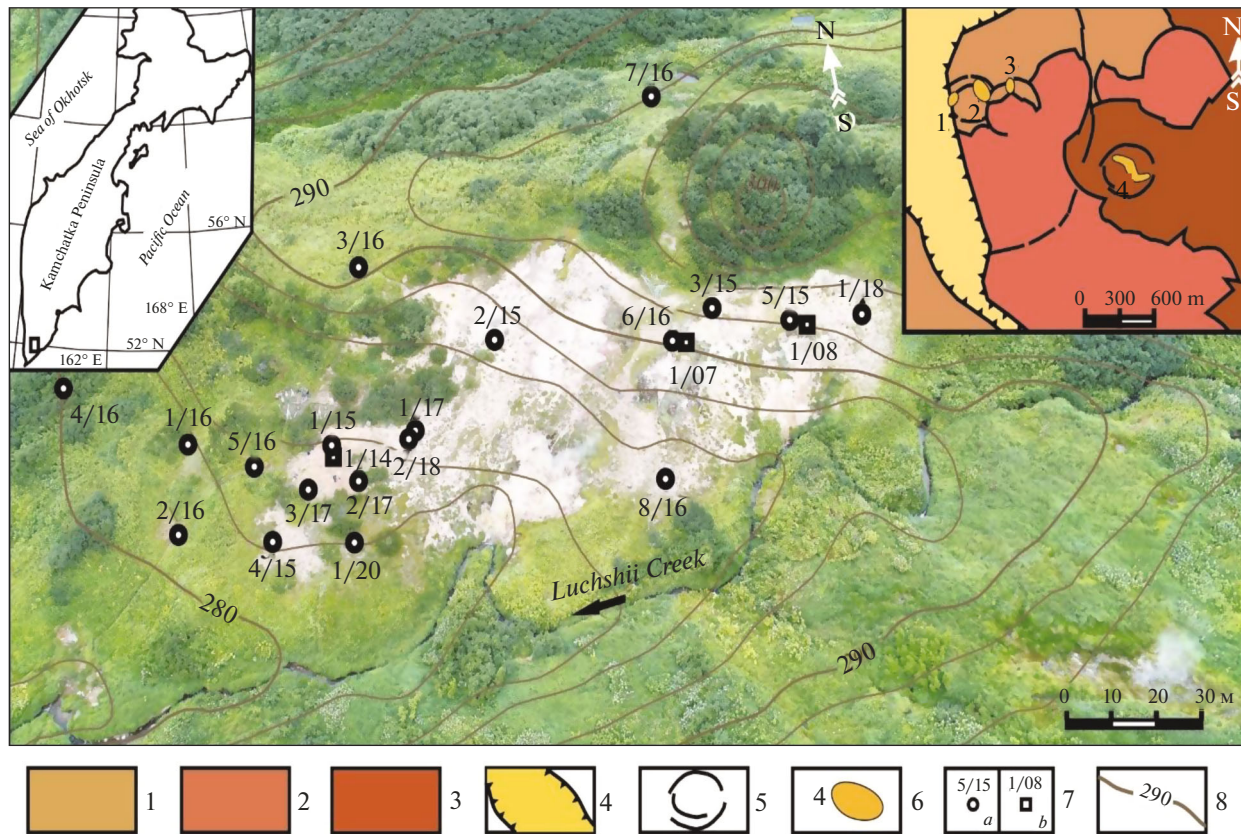


Fig. 1. The East Pauzhetka thermal field: an orthophoto with workings. The insets show the outline of Kamchatka and a simplified geological structure of the Pauzhetka hydrothermal system. (1) Upper Pauzhetka subformation; (2) extrusive lava complex of dacites and rhyolites at the Kambalny mountain range; (3) same, for basaltic andesites at the Kambalny mountain range; (4) Upper Quaternary Pauzhetka graben; (5) outlines of uplifted tectono-magmatic ring blocks; (6) thermal fields: (1) South Pauzhetka field, (2) Upper Pauzhetka field, (3) Lower Pauzhetka field, (4) East Pauzhetka field; (7) workings: (a) core boreholes, (b) pits; (8) absolute heights and relief isolines.

and BaSO_4 (Ba). The analyses were performed with full compliance with all the standard requirements: accelerating voltage 20 kV and the current through the control standard Ni 700 pA, the working distance 15 mm, and the tube diameter size of 2–4 mm. We investigated polished sections and relief surfaces of the samples. Carbon spray coating was used.

Diffractograms of samples were recorded using a MaxRD 7000 X-ray diffractometer (Shimadzu) in the range 6° – $65^\circ 2\theta$, at a step of $0.1^\circ 2\theta$, with a scanning rate of 2 deg./min, which is equivalent to exposure at the point 3 s. The unit cell parameters were estimated using the Rietveld method, which consists in refining the profile parameters of diffractograms in the PowderCell 2.4 program. Oscillatory spectra were obtained using an IRAffinity-1 infrared spectrophotometer with the Fourier transform (Shimadzu), in the wavenumber range 400 – 4000 cm^{-1} , resolution 4 cm^{-1} , and the number of scans 100. Analytical measurements were carried out at the Institute of Volcanology and Seismology FEB RAS (Petropavlovsk-Kamchatsky), Analysts M.A. Nazarova and A.V. Sergeeva.

THE SPECIES COMPOSITION OF ZEOLITES SAMPLED IN THE EAST PAUZHETKA THERMAL FIELD

Zeolite mineralization occurs in all horizons of the mudstone sequence in the thermal field, except for the upper horizon which is composed of kaolinite clays of sulfuric acid leaching (Fig. 3). The zeolite deposits are white in color, frequently because calcite is involved. The maximum amount of zeolites is recorded in the transition zone from montmorillonite “blue clays” to argillized andesites, and in the strongly altered andesites themselves where they replace up to 20–30% of rock volume. Zeolites are localized in the form of isolated features of irregular shape up to 3–5 cm across; they are deposited on the walls of cavities and cracks as crystal crusts and druses up to 0.6 mm across; they fill pores, cavities, and cracks of varying configurations and thickness, as well as occurring in the form of minute crystals and features of irregular shapes. A dense network of zeolite veinlets and the material that fills the space between rock clasts emphasize the breccia-like structure of the andesites.

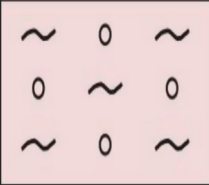
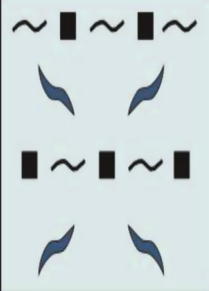

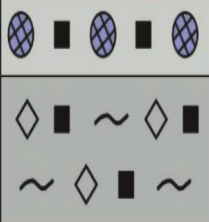
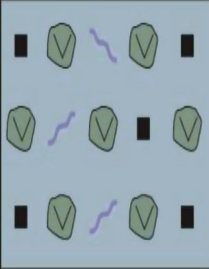

<i>H</i> , cm	Lithologic column	Brief characterization of horizons
100		Clays in the zone of sulfuric acid leaching: kaolinite, opal, α -quartz, sulfates of Ca and Fe; others (see text). Relatively dry and semi-solid.
200		Clays in the zone of carbon dioxide leaching, "blue clay"; montmorillonite (smectites), silica minerals, sulfides. Plastic, ranging from semi-solid to soft plastic, occasionally showing cryptoliquid consistency. Abundance of lenses, veinlets, geodes with opal, α -quartz, and sulfides.
300		Smectite clays with phosphates of Al, Fe, Sc, ... and sulfides.
400		Zone with silica—carbonate-sulfide mineralization. Smectite clay with abundant andesite clasts, opal fragments, pyritized. Dry and solid.
500		Metasomatic breccias in andesite with veinlets and zones of intensive hydrothermal alteration.
600		Original andesites with veinlets and zones of intensive hydrothermal alteration.
700		
800		

Fig. 2. A generalized section of the EPF argillized rocks (after Rychagov et al., 2019) with inaccuracies removed).

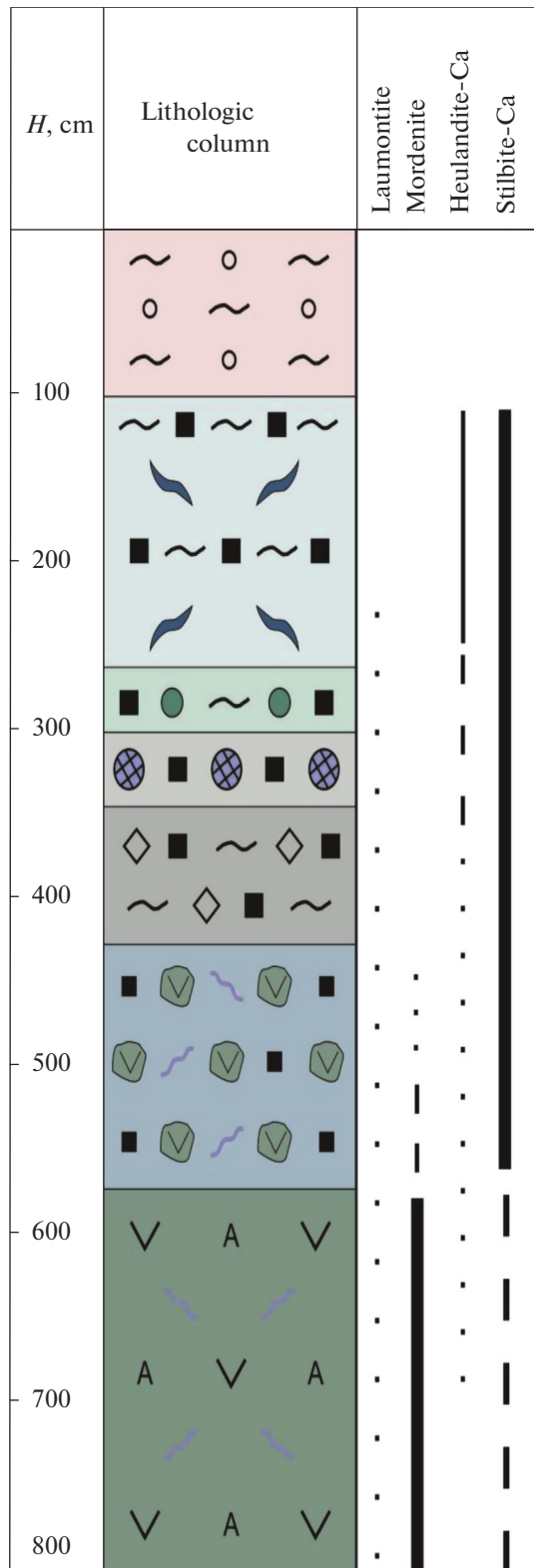


Fig. 3. The distribution of zeolite minerals in the section of the EPF argillized rocks. For a brief description of the layers see Fig. 2.

Laumontite $\text{Ca}_4[\text{Al}_8\text{Si}_{16}\text{O}_{48}]\cdot 18\text{H}_2\text{O}$ is present in mudstones in small amounts. It mostly occurs in plagioclase, as well as making crystals of its own in altered rocks. It occasionally occurs in cavities in the form of bunches of acicular crystals with elongate prismatic habitus up to 3 mm across (Fig. 4a). Veined laumontite is observed as dense accumulations of short prismatic wedge-shaped crystals with perfect cleavage up to 0.1 mm in length in a mass composed of stilbite-Ca in association with opal. We probably observe here several generations of laumontite, which is characteristic for zeolitized propylites found in the Puzhetka HS (Korobov, 2019).

We determined the unit cell parameters for laumontite crystals found in the cracks and cavities of argillized andesites at a depth of about 7 m; these are: $a = 14.72 \text{ \AA}$, $b = 13.08 \text{ \AA}$, $c = 7.56 \text{ \AA}$, $\beta = 112.0^\circ$. Laumontite shows a pronounced crystallinity which can be seen as distinct reflexes in a diffractogram (Fig. 5). The structure of this zeolite was found to contain a high concentration of tetrahedrally oriented aluminum, which is seen in the shape of the infrared spectrum. Among other things, we observe distinct bands around 765 , 960 , and 968 cm^{-1} , which resulted from a $[\text{AlO}_4]$ fragment and constitute a distinguishing feature in the spectra of laumontite and zeolite of this type (Sergeeva, 2019).

Mordenite $(\text{Na}_2, \text{K}_2, \text{Ca})_4[\text{Al}_8\text{Si}_{40}\text{O}_{96}]\cdot 28\text{H}_2\text{O}$ is widely abundant in argillized andesite. It fills veinlets and cavities between rock clasts in the form of sheaf-like acicular colorless crystals or white aggregates. Some individual crystals are as long as 1 mm (see Fig. 4b). In the earlier veinlets mordenite associates with chlorite, while in later ones the association is with montmorillonite, quartz, stilbite-Ca, calcium hydrosilicate (probably okenite), and carbonate.

In diffractograms mordenite is identified from an intensive, but diffused reflex (110) around $6.4^\circ 2\theta$ (see Fig. 5). The other mordenite reflexes are poorly discernible and provide no clue to more accurate determination of the unit cell parameters. The fact that the reflexes are diffuse provides evidence of a low degree of crystallization in the mineral. The main absorption bands for mordenite in the infrared spectrum are around 453 , 1053 , 1177 , 1222 , 3450 , and 3600 cm^{-1} . Mordenite differs from the other zeolites by the absorption profile in the region of valent oscillation of water molecules, $3000\text{--}3650 \text{ cm}^{-1}$, and by the presence of distinct bands around 1177 and 1222 cm^{-1} . In the region $3000\text{--}3650 \text{ cm}^{-1}$, its band consists of two broad components of comparable intensities with maxima around 3600 and 3450 cm^{-1} . In the region of valent and deformation oscillations of tetrahedra $[(\text{Al}, \text{Si})\text{O}_4]$, below 1200 cm^{-1} , its spectrum contains two intensive bands around 1053 ($\nu(\text{SiO}_4)$) and 453 ($\delta(\text{SiO}_4)$) cm^{-1} , as well as a series of less intensive bands.

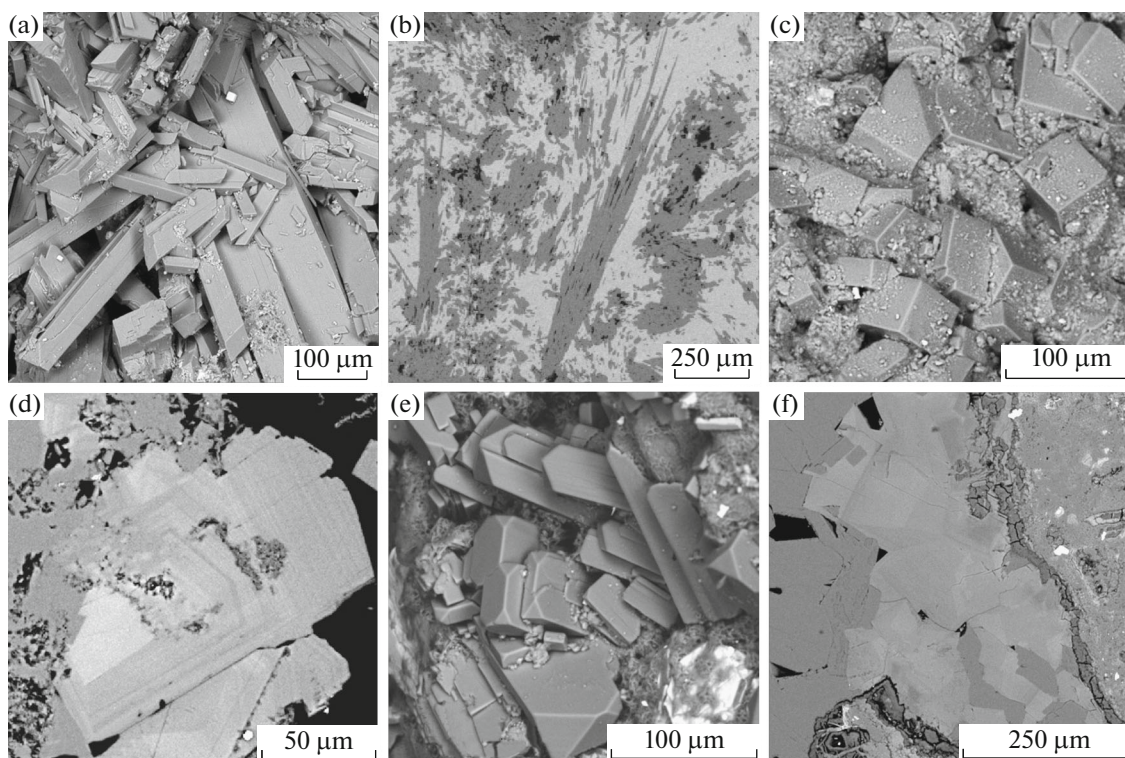


Fig. 4. The morphology and internal structure of zeolites from the EPF mudstones. (a) prismatic laumontite crystals in argillized andesite, depth 7 m; (b) acicular mordenite crystals (grey) in calcite (white), polished section; (c) heulandite-Ca crystals in a smectite mass; (d) zonal heulandite-Ca crystals that overgrow stilbite-Ca (grey) on the wall of a crack (polished section), core and light-colored zones in heulandite-Ca are enriched in barium; (e) stilbite-Ca crystals in a smectite mass (the white grains consist of pyrite); (f) stilbite-Ca (grey on the left) in intergrowth with zonal heulandite-Ca (light grey tints in the middle) fill in a veinlet in altered andesite (polished section), smectite (dark grey) is the veinlet along the boundary. BSE images.

Heulandite-Ca $(\text{Na,K})\text{Ca}_4[\text{Al}_9\text{Si}_{27}\text{O}_{72}]\cdot 24\text{H}_2\text{O}$ occurs widely, but in low amounts. More frequently, the mineral is encountered in veinlets and cavities of “blue clay” together with stilbite-Ca. Heulandite-Ca typically has an isometric habitus of its crystals whose size does not exceed 0.15 mm (see Fig. 4c). When cut, crystals have a trapeziform shape, a sectoral or zonal structure, which is due to different relationships between elements such as Mg, Sr, Ba, and K in zones and sectors (see Fig. 4d). Less siliceous zones have concentrations of Sr, Ba, and K nearly twice as high as those in high-silica zones, with about the same concentration of Ca. Heulandite-Ca crystallizes later than stilbite-Ca does, filling in the space between the crystals of the latter and in part replacing it. When the replacement occurs in lighter-colored zones along the edge of stilbite-Ca, one observes barium (up to 1.3 wt % BaO).

We obtained diffractograms and infrared spectra of heulandite-Ca from those samples which were taken within local exposures of altered rocks at the surface of the thermal field (see Fig. 5). The unit cell parameters for heulandite-Ca based on the position of reflexes in the diffractogram are as follows: $a = 17.63 \text{ \AA}$, $b = 17.82 \text{ \AA}$, $c = 7.40 \text{ \AA}$, and $\beta = 116.5^\circ$. Judging by the unit cell

parameters, this heulandite-Ca is similar to naturally occurring heulandites that contain Ca, Sr, Ba, K, and Na (Seryotkin, 2015). The infrared spectrum for heulandite-Ca involves pronounced bands around 462, 1056, 3430, and 3620 cm^{-1} . Unlike the mordenite spectrum, there are no distinct bands around 1177 and 1222 cm^{-1} , while the absorption in the range 3000–3650 cm^{-1} is asymmetrical, with the band around 3430 cm^{-1} having greater intensity compared with that around 3620 cm^{-1} .

Stilbite-Ca $\text{NaCa}_4[\text{Al}_9\text{Si}_{27}\text{O}_{72}]\cdot 30\text{H}_2\text{O}$ is the most abundant mineral of the zeolite group in mudstones. It is deposited in cracks and on the surface of cavities as flattened semitransparent, well-shaped tabular crystals, as well as their growths, druses, and parallel laminated aggregates (see Figs. 4e, 4f). Stilbite-Ca crystals reach lengths of 0.6 mm and have different habitus shapes, ranging from elongate thin-laminated and tabular to isometric thick-plate shapes. The surface of crystals occasionally shows traces of dissolution.

When encountered in the cementing mass of argillized andesite breccias, the mineral occurs as continuous masses, parallel coalesced plates, short- and long-columnar or wedge-shaped crystals and aggregates, or as split sheaf-like or radial features. In the earlier vein-

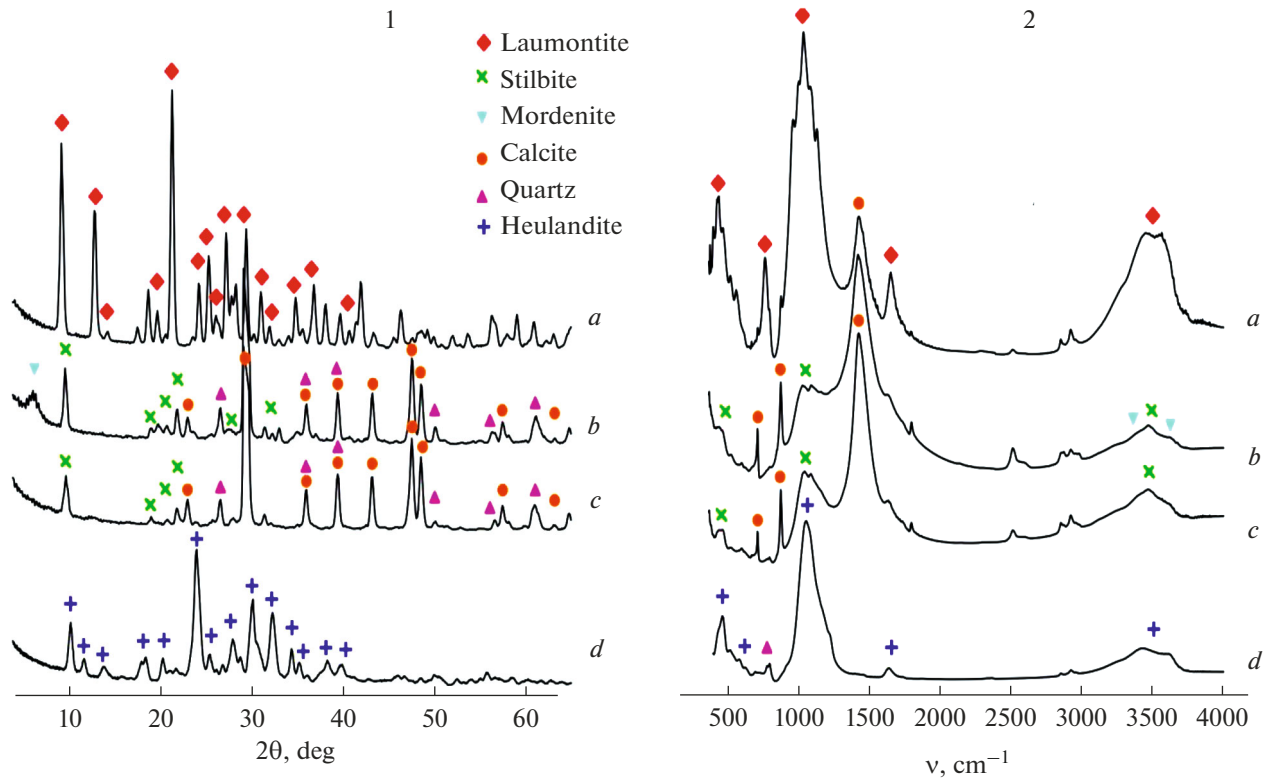


Fig. 5. Diffractograms (1) and infrared spectra (2) for laumontite (*a*), stilbite-Ca, and mordenite in association with quartz and magnesium-bearing calcite (*b*), stilbite-Ca in association with quartz and magnesium-bearing calcite (*c*), heulandite-Ca with quartz (*d*) from EPF mudstones.

lets, stilbite-Ca associates with chlorite, while in the later thick veinlets one can observe, from edge to center, consecutively deposited montmorillonite, stilbite-Ca, heulandite-Ca, chalcedony (or quartz), and calcite.

The unit cell parameters in stilbite-Ca are as follows: $a = 13.62 \text{ \AA}$, $b = 18.26 \text{ \AA}$, $c = 11.28 \text{ \AA}$, $\beta = 127.8^\circ$. These parameters are consistent with a stilbite-Ca of the composition $\text{Ca}_{3.5}\text{Na}(\text{Si}_{28}\text{Al}_8\text{O}_{72})(\text{H}_2\text{O})_{40}$, but there can also be other exchange cations (K, Mg, Ba, Sr, among others). The infrared spectra for samples with stilbite-Ca show bands corresponding to oscillations of tetrahedral aluminum; they are very weak, and superposed upon quartz bands (see Fig. 5). The absorption curve in the range $3000\text{--}4000 \text{ cm}^{-1}$ shows the difference between the spectra of stilbite-Ca and of laumontite. For laumontite we have two broad bands of high intensity peaking at 3460 and 3560 cm^{-1} , while the spectrum of stilbite-Ca contains a single comparatively narrow band at 3620 cm^{-1} and a broader band peaking at 3460 cm^{-1} . The diffractograms show magnesium-bearing calcite in association with zeolites. This differs from pure calcite in having reflexes displaced toward greater angles.

THE CHEMICAL COMPOSITION OF ZEOLITES SAMPLED IN THE EAST PAUZHETKA THERMAL FIELD AS REVEALED BY ENERGY DISPERSIVE SPECTROMETRY

The electron probe analysis has certain limitations in the study of zeolite minerals. However, the study of zeolites sampled in alkaline massifs worldwide showed that rocks of different series that were generated nearly at the same time, including those capable of polymorphism, can be clearly distinguished from relationships between dominant or important accessory components (Pekov et al., 2004). Calculation applied to electron probe analyses of these zeolites showed generally fairly good results for stoichiometry, charge balance, and total deficit. The results of our study enable us to state that this is also true with regard to the zeolites sampled in the present-day Puzhetka HS.

Preliminary analysis of zeolite compositions showed that the EPF zeolites are medium- (2–3) and high-silica (>3) calcium varieties, judging from the ratio of atomic abundances Si/Al (2.05–5.31) and from the concentration of the main component (CaO, wt %). The Si/Al–CaO diagram shows the zeolite compositions to divide into four groups (Fig. 6). In the first group, the concentration of CaO varies in the range 8.75–12.36 wt %, and that of Si/Al varies in the

range 2.02–2.34. In the second group we have CaO 3.84–5.52 and Si/Al 4.23–5.29; in the third, CaO 4.44–7.01 and Si/Al 2.75–3.80; and in the fourth, CaO 6.13–9.25 and Si/Al 2.83–4.28. The compositional areas of the two groups with the concentration of CaO 6.13–7.01 wt % partially overlap. In such a case, analyses were classified as belonging to a group based on morphology and internal structure of the mineral. In this way the minerals were determined to be laumontite, mordenite, heulandite-Ca (Si/Al < 4.0), and stilbite-Ca by chemical composition, morphology, and internal structure. The identification of these types of zeolite was confirmed using methods of X-ray diffractometry and infrared spectrometry.

We calculated the chemical composition of minerals using the maximum possible number of analyses (1272): 79 laumontite analyses, 108 mordenite analyses, 103 heulandite-Ca analyses, and 973 stilbite-Ca analyses. We eliminated from the calculation those analyses which showed significant deviations from stoichiometry where the charge balance exceeded 10% on both sides (Passaglia, 1970; Passaglia and Sheppard, 2001). The typical zeolite composition is shown in Table 2. The average zeolite composition and the limits of variation for the concentrations of dominant components are listed in Table 3.

The composition of the zeolite framework is characterized by the quantity $T_{Si} = Si/(Si + Al + Fe)$, which shows the percentage of tetrahedra that are occupied by Si (Coombs et al., 1997; Passaglia, 1970; Passaglia and Sheppard, 2001). Most zeolites have the average value of T_{Si} above those in the empirical formulas. For laumontite we have T_{Si} equal to 0.69, while the corresponding value in the empirical formula is 0.67; for heulandite-Ca we have 0.76 as against 0.75; for stilbite-Ca, 0.77 as against 0.75 (see Table 3). The value for mordenite is slightly lower, 0.82 as against 0.83. The range of T_{Si} for all EPF zeolites is coincident with that characteristic for zeolites of these species, except that the maximum value of T_{Si} for stilbite-Ca is slightly higher, reaching 0.81 as against 0.78 (Coombs et al., 1997; Passaglia and Sheppard, 2001). Deviations in the composition of naturally occurring zeolites can be due to a number of factors, including structural peculiarities of the zeolites, as well as to the presence in them of “superfluous” anions or to cations that cannot be determined by electron probe techniques (H^+ or H_3O^+) (Pekov et al., 2004).

Zeolites have variable degrees of orderliness in the distribution of Al and Si in the framework, expressible in terms of the Si/Al ratio. For laumontite with an ordered distribution, the values of Si/Al are compact in the diagram, mordenite and heulandite-Ca with partially ordered distributions have a wider area, while the largest variations in Si/Al are observed in stilbite-Ca with an unordered distribution of framework cations (Fig. 7). As well, the Si/Al distribution for heulandite-Ca has two trends, a “silica” trend and an

“aluminum” trend, which is probably due to the zonal structure of this mineral. Overall, the values of T_{Si} and Si/Al for the EPF zeolites indicate that laumontite, heulandite-Ca, and stilbite-Ca are enriched in silica, while mordenite is enriched in aluminum.

The non-framework cations in zeolites are Mg, Ca, Sr, Ba, Na, and K. The concentration of Ca is the greatest in laumontite, 10.16 wt % CaO on average. The next to follow are stilbite-Ca (7.68), heulandite-Ca (6.18), and mordenite (4.87 wt% CaO). The calculation of the stilbite-Ca formula shows that the mineral is similar (as to the concentration of calcium) to stellerite with its formula $Ca_4[Al_8Si_{28}O_{72}] \cdot 28H_2O$ (Passaglia and Sheppard, 2001), which is a pure calcium member in the isomorphous series of the structural stilbite group. However, a reliable classification of stellerite requires additional accurate X-ray structural analysis.

The zeolites are sufficiently well identifiable from the concentrations of accessory cations. The admixtures of accessory cations in laumontite are unstable and very low: 0.01 for MgO, 0.01 for SrO, 0.01 for BaO, 0.16 for Na₂O, and 0.38 wt % for K₂O. Mordenite contains a substantial amount of Na (1.43 wt% Na₂O on average), with episodic appearances of Sr (up to 1.11 wt% SrO). Heulandite-Ca is the main concentrator of Mg, Ba, and K (the average values are 0.58 wt % MgO, 1.37 BaO, and 0.59 K₂O), while some individual zones in it are enriched in Sr (0.53 wt % SrO on average). The zones with less silica have higher concentrations of K, Ba, and Sr with about the same amount of Ca in all zones. The average concentrations of accessory cations in stilbite-Ca are unstable and low, but are higher on average than in laumontite: MgO 0.07, SrO 0.15 wt %, BaO 0.06, Na₂O 0.15, and K₂O 0.24 wt % (see Table 3). The differences between zeolites in the composition of non-framework cations are the most pronounced in the Na–K–Sr diagram (Fig. 8). The overall sequence of cation accumulation in the EPF zeolites over time looks as follows: Ca + K (laumontite) → Ca + Na (mordenite) → Ca + K + Na + Sr (stilbite-Ca) → Ca + Ba + K + Mg + Sr (heulandite-Ca). The elements are arranged in decreasing order.

The calculated average amount of water in zeolites is in general agreement with that given by the formulas (see Table 3). The range of values for calculated amount of water is wide enough for laumontite, mordenite, and stilbite-Ca, which could be due to the habitus shapes of the crystals. As an example, the analyses performed along the elongation of acicular mordenite crystals show that the concentration of water there is lower than that in analyses across the crystals.

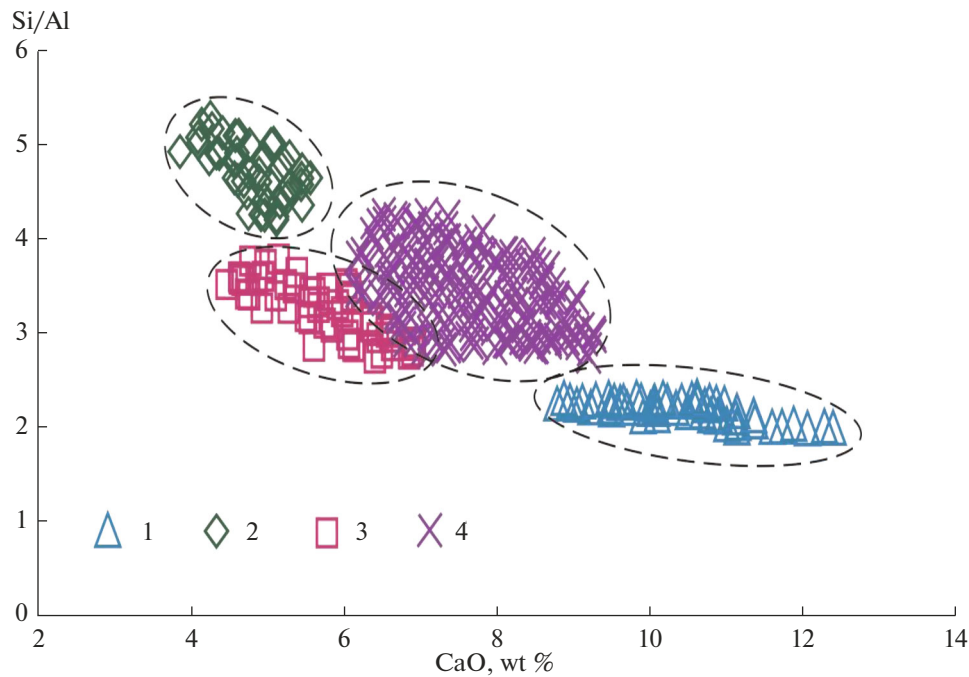


Fig. 6. The Si/Al ratio (atomic amounts) and CaO (wt%) in zeolites from the EPF mudstones. (1) laumontite; (2) mordenite; (3) heulandite-Ca; (4) stilbite-Ca. Dashed lines enclose compositional areas for various zeolite species.

THE CONDITIONS OF FORMATION FOR ZEOLITES IN THE EAST PAUZHETKA THERMAL FIELD

The occurrence of zeolite mineralization in rocks of the Puzhetka HS shows an overall agreement with vertical metasomatic zonation, and is controlled by the temperature and chemical composition of the thermal solutions, by their salinity and pH (Naboko, 1963; Naboko et al., 1965; Korobov et al., 1992; *Struktura ...*, 1993). According to the ideas advanced by A.D. Korobov, in a present-day hydrothermal system the zeolite facies is part of the argillization zone in the region where vapor-dominated hydrothermal fluids are discharged (Korobov, 2019).

We know that the temperatures of rocks and geothermal heat carrier in the present-day Puzhetka HS reach 200–220°C (Belousov et al., 1976; *Struktura ...*, 1993). Accordingly, argillization occurs at temperatures that do not exceed these. A study of liquid–gas inclusions in secondary minerals showed (Korobov, 2019) that vein calcite that frequently associates with zeolites forms at temperatures of 50–170°C, clinoptilolite (heulandite?) at 80–110°C, mordenite at 90–135°C, while the low-temperature β -leopardite (laumontite) at 170–180°C.

The temperature of a “blue clay” core from the EPF section (depth 2–4 m) is 70–98°C. The temperature of the underlying argillized andesites is higher, 105–110°C, and can apparently reach 150°C. The data on the temperature profile in the EPF argillization zone are consistent with the sequence of zeolite depo-

sition and their distribution over the section. The lower section (at depths of 6–10 m), at a comparatively elevated temperature, is dominated by mordenite. Stilbite-Ca occurs throughout the entire section, but is deposited later than mordenite is, while heulandite-Ca is deposited later than stilbite-Ca and is observed in considerable amounts in the upper section only. Laumontite is encountered episodically throughout the entire section, but more frequently in the lower layers of the shallow argillization zone. Previous data tell us that laumontite is especially abundant in permeable tuffs of the Middle and Lower Puzhetka subformation (at depths between 100–120 and 500 m) with stratal water temperature $\leq 200^\circ\text{C}$, where it replaces up to 50–60% of altered rock (Lebedev, 1979; Naboko et al., 1965; Naboko, 1980; *Struktura ...*, 1993). Based on experimental data, the metasomatic boundary between the laumontite zone and the zone where stilbite is formed at a low $P_{\text{H}_2\text{O}}/P_{\text{total}}$ ratio and the presence of NaCl, CO_2 , and S in the liquid phase is at a temperature below 150°C (Liou, 1971). Accordingly, this explains the dominance of laumontite where hydrothermal metasomatic alteration of tuffs occurs in the Middle and Lower Puzhetka subformations.

The hydrothermal fluids of the Puzhetka HS as reached by deep drillholes are near neutral or alkaline (pH = 7.0–8.2) and chloride-sodium mineralized (up to 2.8–4.1 g/L); they are enriched in carbon dioxide and hydrogen sulfide and contain higher concentrations of silicic acid (up to 0.8 g/L); total alkali metals

Table 2. The chemical composition of the zeolites from the EPF mudstones as revealed using energy dispersive spectrometry (wt %)

Mineral	Laumontite			Mordenite			Heulandite-Ca			Stilbite-Ca		
Component	1	2	3	4	5	6	7	8	9	10	11	12
SiO ₂	51.39	51.82	49.06	65.74	65.98	67.34	56.94	56.52	57.20	59.00	58.14	57.83
Al ₂ O ₃	20.56	21.72	20.63	11.42	11.72	11.55	16.15	16.18	15.85	14.18	16.27	14.94
Fe ₂ O ₃	—	—	—	—	—	—	—	—	—	—	0.53	—
MgO	—	—	—	—	—	—	0.76	0.11	—	0.09	0.12	—
CaO	10.75	12.36	11.69	4.22	4.86	4.35	6.02	6.42	6.97	7.86	7.88	7.68
SrO	—	—	—	—	—	0.66	0.76	0.92	0.91	—	—	—
BaO	—	—	—	—	—	—	1.76	2.51	1.52	—	—	—
Na ₂ O	0.27	—	—	1.74	1.71	1.77	—	0.14	—	0.07	0.28	0.33
K ₂ O	0.14	—	—	0.29	0.19	0.19	0.89	0.82	0.78	—	0.67	—
Total	83.11	85.90	81.38	83.41	84.46	85.86	83.28	83.62	83.23	81.20	83.89	80.78

Formula coefficients

	calculation for O ₄₈			calculation for O ₉₆			calculation for O ₇₂					
Si	16.33	16.01	16.00	39.92	39.67	39.90	27.02	26.97	27.18	28.00	27.01	27.64
Al	7.71	7.92	7.94	8.18	8.31	8.08	9.04	9.11	8.89	7.94	8.92	8.42
Fe	—	—	—	—	—	—	—	—	—	—	0.18	—
Σ f.a.	24.04	23.93	23.94	48.10	47.98	47.98	36.06	36.08	36.06	35.94	36.11	36.06
Mg	—	—	—	—	—	—	0.54	0.08	—	0.06	0.08	0
Ca	3.66	3.99	4.09	2.75	3.13	2.76	3.06	3.28	3.55	4.00	3.92	3.93
Sr	—	—	—	—	—	0.23	0.21	0.25	0.25	—	—	—
Ba	—	—	—	—	—	—	0.33	0.47	0.28	—	—	—
Na	0.17	—	—	2.05	1.99	2.03	—	0.13	—	0.06	0.25	0.31
K	0.06	—	—	0.22	0.15	0.14	0.54	0.50	0.47	—	0.40	—
Σ non c.	3.88	3.99	4.09	5.02	5.27	5.17	4.67	4.71	4.55	4.12	4.65	4.24

Σ f.a. means total framework atoms, Σ non c. stands for total non-framework cations.

in these are much higher than alkaline-earth metals, while the concentration of Sr reaches 1.1 mg/L (Pampura, 1980). One of the more important non-framework cations in zeolites is Ba, which is considered to be a deep-seated element, similarly to Sr. According to an analysis performed by us at the Institute of Geochemistry, Siberian Branch, RAS using the ICP–MS technique (Analyst G.P. Sandimirova), the concentration of Ba in the water flowing from well GK-3 reaches 0.053 mg/L.

It is thought that the EPF thermal waters are various condensates (Pampura, 1977). Shallow condensates of vapor-dominated gas jets in the middle of the field are bicarbonate ammonium calcium waters of low salinity (0.035–0.2 g/L), with pH = 7–8, while the concentration of Sr in them varies between 0.1 and 0.6 mg/L. They contain large amounts of dissolved carbon dioxide and hydrogen sulfide (CO₂ 0.265–0.348 g/L, H₂S 0.039–0.073 g/L). The shallow

condensates from mud funnels are more acidic (pH = 3–4), they have a sulfate ammonium magnesium-calcium composition with a salinity that reaches 0.7 g/L, and high concentrations of iron, zinc, and silicic acid. The total alkaline-earth metals in the condensates dominate over alkaline metals. We know that the condensate waters in the discharge zone of the hydrothermal system are formed under the influence of freely circulating waters, including ascending pressure-driven solutions (Pampura, 1977). Taking the example of the EPF, as well as of the South Kambalny Central Thermal Field, we showed that the zones of carbonatization and zeolitization, as well as zones with phosphate and silica–carbonate–sulfide mineralization at the bottom of the hydrothermal clay sequence, are generated by supply of alkaline thermal waters coming from depth, by their boiling and apparently active mixing with condensates of vapor-dominated gas jets (Rychagov et al., 2017, 2021).

Table 3. The average composition of EPF zeolites inferred from results of energy dispersive spectrometry (wt %)

Mineral*	Laumontite	Mordenite	Heulandite-Ca	Stilbite-Ca
Formula**	$\text{Ca}_4[\text{Al}_8\text{Si}_{16}\text{O}_{48}] \cdot 18\text{H}_2\text{O}$	$(\text{Na}_2, \text{K}_2, \text{Ca})_4[\text{Al}_8\text{Si}_{40}\text{O}_{96}] \cdot 28\text{H}_2\text{O}$	$(\text{Na}, \text{K})\text{Ca}_4[\text{Al}_9\text{Si}_{27}\text{O}_{72}] \cdot 24\text{H}_2\text{O}$	$\text{NaCa}_4[\text{Al}_9\text{Si}_{27}\text{O}_{72}] \cdot 30\text{H}_2\text{O}$
Structural type**	LAU	MOR	HEU	STI
Orderliness of Si and Al**	O	P	P	U
1	2	3	4	5
SiO ₂	$\frac{51.10}{48.39-54.56}$	$\frac{65.01}{62.21-69.00}$	$\frac{58.02}{54.82-62.83}$	$\frac{58.28}{52.65-66.49}$
Al ₂ O ₃	$\frac{19.55}{18.27-22.18}$	$\frac{11.75}{10.61-13.01}$	$\frac{15.44}{13.61-17.63}$	$\frac{14.41}{12.33-17.16}$
Fe ₂ O ₃	$\frac{0}{0-0.11}$	$\frac{0.01}{0-0.63}$	$\frac{0}{0-0}$	$\frac{0.03}{0-1.00}$
MgO	$\frac{0.01}{0-0.12}$	$\frac{0.01}{0-0.36}$	$\frac{0.58}{0-1.95}$	$\frac{0.07}{0-0.96}$
CaO	$\frac{10.21}{8.75-12.36}$	$\frac{4.87}{3.84-5.52}$	$\frac{6.18}{4.44-7.01}$	$\frac{7.68}{6.13-9.25}$
SrO	$\frac{0.01}{0-0.57}$	$\frac{0.28}{0-1.11}$	$\frac{0.53}{0-1.35}$	$\frac{0.15}{0-1.98}$
BaO	$\frac{0.01}{0-0.14}$	$\frac{0.01}{0-0.26}$	$\frac{1.37}{0.24-3.19}$	$\frac{0.06}{0-1.57}$
Na ₂ O	$\frac{0.16}{0-0.38}$	$\frac{1.43}{0.47-2.15}$	$\frac{0.05}{0-0.26}$	$\frac{0.15}{0-0.86}$
K ₂ O	$\frac{0.38}{0-0.92}$	$\frac{0.22}{0-0.59}$	$\frac{0.59}{0.13-0.98}$	$\frac{0.24}{0-1.25}$
Total	$\frac{81.43}{77.07-87.20}$	$\frac{83.59}{80.37-87.81}$	$\frac{82.77}{79.18-86.43}$	$\frac{81.12}{74.40-89.82}$
D.T.A.	$\frac{18.57}{12.80-22.93}$	$\frac{16.41}{12.19-19.63}$	$\frac{17.23}{13.57-20.82}$	$\frac{18.48}{10.18-25.60}$
H ₂ O	$\frac{20.18}{12.98-26.13}$	$\frac{33.43}{23.62-41.46}$	$\frac{27.27}{26.52-28.59}$	$\frac{29.49}{14.57-44.18}$
Si	$\frac{16.56}{16.00-16.84}$	$\frac{39.56}{38.59-40.46}$	$\frac{27.46}{26.52-28.59}$	$\frac{27.70}{26.41-29.08}$
Al	$\frac{7.47}{7.17-7.96}$	$\frac{8.44}{7.66-9.15}$	$\frac{8.63}{7.52-9.66}$	$\frac{8.08}{6.80-9.41}$
Fe ⁺⁺⁺	$\frac{0}{0-0.03}$	$\frac{0.01}{0-0.29}$	$\frac{0}{0-0}$	$\frac{0.01}{0-0.35}$
Mg	$\frac{0.01}{0-0.06}$	$\frac{0.01}{0-0.34}$	$\frac{0.41}{0-1.31}$	$\frac{0.05}{0-0.68}$
Ca	$\frac{3.55}{3.12-4.09}$	$\frac{3.18}{2.55-3.53}$	$\frac{3.14}{2.22-3.58}$	$\frac{3.91}{3.14-4.75}$

Table 3. (Contd.)

Mineral*	Laumontite	Mordenite	Heulandite-Ca	Stilbite-Ca
Formula**	$\text{Ca}_4[\text{Al}_8\text{Si}_{16}\text{O}_{48}] \cdot 18\text{H}_2\text{O}$	$(\text{Na}_2, \text{K}_2, \text{Ca})_4[\text{Al}_8\text{Si}_{40}\text{O}_{96}] \cdot 28\text{H}_2\text{O}$	$(\text{Na}, \text{K})\text{Ca}_4[\text{Al}_9\text{Si}_{27}\text{O}_{72}] \cdot 24\text{H}_2\text{O}$	$\text{NaCa}_4[\text{Al}_9\text{Si}_{27}\text{O}_{72}] \cdot 30\text{H}_2\text{O}$
Structural type**	LAU	MOR	HEU	STI
Orderliness of Si and Al**	O	P	P	U
1	2	3	4	5
Sr	$\frac{0}{0-0.11}$	$\frac{0.10}{0-0.40}$	$\frac{0.15}{0-0.37}$	$\frac{0.05}{0-0.54}$
Ba	$\frac{0}{0-0.02}$	$\frac{0}{0-0.06}$	$\frac{0.25}{0.04-0.60}$	$\frac{0.01}{0-0.30}$
Na	$\frac{0.10}{0-0.24}$	$\frac{1.69}{0.57-2.50}$	$\frac{0.05}{0-0.24}$	$\frac{0.13}{0-0.76}$
K	$\frac{0.15}{0-0.37}$	$\frac{0.17}{0-0.47}$	$\frac{0.36}{0.08-0.60}$	$\frac{0.15}{0-0.77}$
Total	$\frac{27.84}{27.97-27.99}$	$\frac{53.15}{52.54-54.08}$	$\frac{40.44}{39.69-41.08}$	$\frac{40.10}{39.51-41.34}$
$\Sigma_{\text{f.a.}}$	$\frac{24.03}{23.81-24.16}$	$\frac{48.00}{47.78-48.18}$	$\frac{36.08}{35.93-36.20}$	$\frac{35.79}{35.75-36.19}$
$\Sigma_{\text{non c.}}$	$\frac{3.81}{3.53-4.26}$	$\frac{5.15}{4.43-6.28}$	$\frac{4.35}{3.58-5.05}$	$\frac{4.31}{3.38-5.60}$
T_{Si}	$\frac{0.69}{0.67-0.70}$	$\frac{0.82}{0.81-0.84}$	$\frac{0.76}{0.73-0.79}$	$\frac{0.77}{0.74-0.81}$
Si/Al	$\frac{2.22}{2.02-2.34}$	$\frac{4.70}{4.23-5.29}$	$\frac{3.20}{2.75-3.80}$	$\frac{3.43}{2.83-4.28}$
$\text{H}_2\text{O}/\text{f.c.}$	$\frac{0.75}{0.74-0.76}$	$\frac{0.58}{0.58-0.59}$	$\frac{0.67}{0.66-0.67}$	$\frac{0.78}{0.77-0.78}$
FD	17.7	17.2	17.0	16.9
N.A.	79	108	103	973
Ox	48	96	72	72

*Recommended nomenclature of zeolite minerals (Coombs et al., 1997), ** (Gottardi and Galli, 1985; Armbruster and Gunter, 2001). The minerals are arranged in accordance with the classification system adopted by the International Zeolite Association, IZA (Armbruster and Gunter, 2001). The degree of orderliness: O ordered, P partially ordered, U unordered. The figures in the numerator were found as arithmetic means over all analyses of the relevant minerals, the denominator shows variations in the concentration of components. Fe_2O_3 was calculated based on $\text{FeO}_{\text{total}}$. D.T.A. means deficit of total in analyses. The concentration of water (H_2O) is based on the deficit of total analyses. $\Sigma_{\text{non c.}}$ denotes total non-framework cations (Mg + Ca + Ba + Sr + Na + K); $\Sigma_{\text{f.a.}}$ is total framework atoms (Si + Al + Fe). $T_{\text{Si}} = \text{Si}/(\text{Si} + \text{Al} + \text{Fe})$. $\text{H}_2\text{O}/\text{f.c.}$ means the ratio between the number of water molecules in the formula and the number of framework cations. FD stands for framework density (Armbruster and Gunter, 2001). N.A. means the number of analyses for which these data are given. Ox means the number of oxygen atoms in the formula.

Pore solutions form during interaction between fluids coming from below and host rocks, with endogenous minerals being leached out. Consequently, the solutions have a more complex chemical composition, greater salinity (up to 6–7 g/L), and are more enriched in silica (Rychagov et al., 2017). The composition of pore solutions clearly shows two distinct zones in the

thermal field section, one of sulfuric acid leaching and the other of carbon dioxide leaching. The zone of sulfuric acid leaching that is largely composed of kaolinite clays, has its average (median) values of total alkali metals (based on 23 analyses) equal to 0.033 g/L, the respective figure being 0.025 g/L for alkaline-earth metals, and the pH value of the solution is 3.7; one

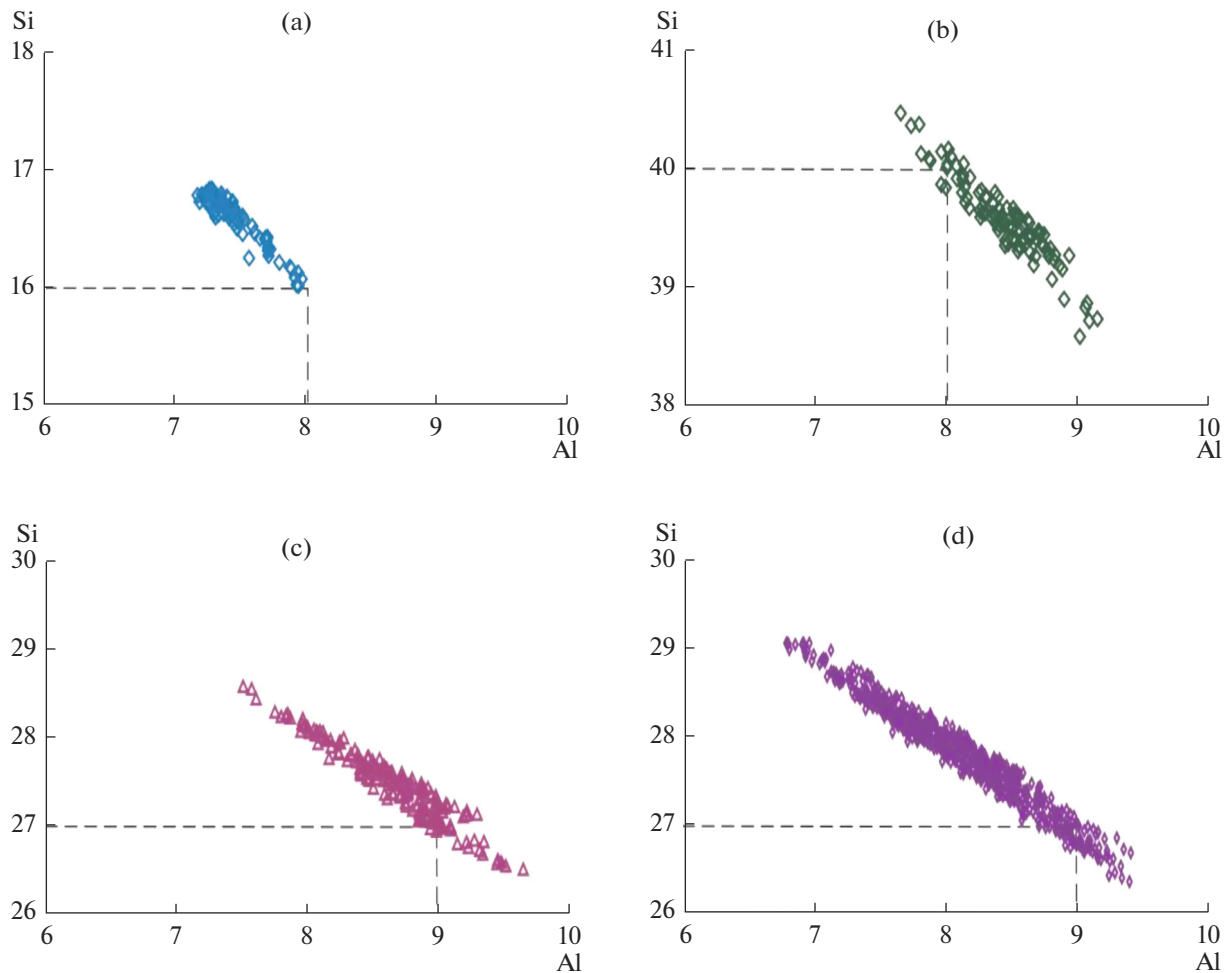


Fig. 7. The relationship between Si and Al (formula units) in laumontite (a), mordenite (b), heulandite-Ca (c), and stilbite-Ca (d) from the EPF mudstones. Dashed lines indicate the “ideal” values: $\text{Al}_8\text{Si}_{16}$ for laumontite, $\text{Al}_8\text{Si}_{40}$ for mordenite, $\text{Al}_9\text{Si}_{27}$ for heulandite-Ca and for stilbite-Ca.

notes a high concentration of iron (0.032 g/L) and a low concentration of ammonium (0.008 g/L) (Table 4). The values of trace elements such as Sr and Ba are 0.19 and 0.24 mg/L, respectively. The total salinity of the solutions is 2.3 g/L.

In the zone of carbon dioxide leaching with dominance of montmorillonite clays and a wide occurrence of zeolite mineralization (stilbite-Ca in the first place), pH increases to reach 7 or higher, the concentration of sulfate ions decreases, and the hydrocarbonate ion starts to dominate whose concentration is 0.6 g/L. The concentrations of chlorine and fluorine increase by factors of three, reaching 0.071 and 0.01 g/L, respectively. The total alkali metals are 0.2 g/L, potassium dominates over sodium compared with their ratio in the overlying horizon. The concentrations of calcium and magnesium rapidly increase, their sum occasionally reaching 0.6 g/L. The values of Sr and Ba also increase in that zone, reaching 0.6 and 0.45 mg/L,

respectively. The total salinity in the solutions is 2.4 g/L on average, but may also rise to 6–7 g/L.

The resulting values of ion concentrations reflect the compositions of those solutions which formed the environment for zeolite generation. One notes a persistent general tendency in the variation of pore solution compositions over the section of the thermal field, namely, increasing concentrations of the components toward the bottom of the clay sequence and preserved values of the concentrations in the argillized andesites. The values of pH and temperature also increase toward the bottom of the section. Accordingly, it is at the bottom of the hydrothermal clay sequence and in the argillized andesites that one observes the most intensive occurrence of zeolite mineralization.

We know that alkaline solutions are used for zeolite synthesis (Mamedova, 2019; Senderov and Khitarov, 1970). In such solutions, the ions $[\text{H}_n\text{SiO}_4]^{n-4}$ and $[\text{Al}(\text{OH})_4]^-$ of tetrahedral coordination make chains

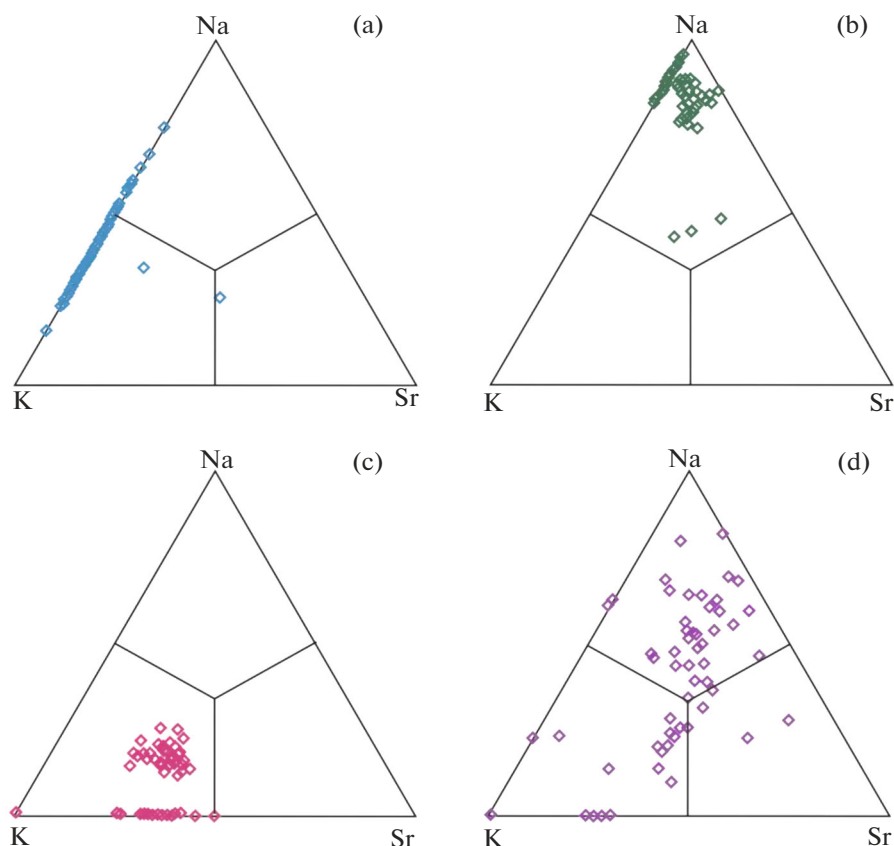


Fig. 8. The relationships between Na, K, and Sr (atomic amounts) in laumontite (a), mordenite (b), heulandite-Ca (c), and stilbite-Ca (d) from the EPF mudstones.

by the mechanism of polycondensation, resulting in heteropolychains being formed; these are initial structural blocks for zeolite frameworks (Iler, 1979; Zhdanov et al., 1981).

The alkalinity of the Pauzhetka field thermal solutions is primarily due to a high concentration of carbonate ions in them. As the water is rising toward the upper horizons of the field, the solutions are being degassed in accordance with $2\text{HCO}_3^- = \text{CO}_2 + \text{CO}_3^{2-} + \text{H}_2\text{O}$. The resulting carbonate ion reacts with water, producing alkalis: $\text{H}_2\text{O} + \text{CO}_3^{2-} = \text{HCO}_3^- + \text{OH}^-$. At high temperatures, if the solution is enriched in carbonate ions and cations of alkali metals (which can be the case in the interior of the Pauzhetka HS due to supply of rare and dominantly alkali elements by thermal water from depth (*Struktura ...*, 1993)), the transformation occurs in a vigorous manner, and pH can reach 10. Such waters are highly aggressive toward many aluminosilicates, but zeolites with moderate amounts of silica (laumontite, among others) are stable enough (Koporulin, 2013). In the Pauzhetka HS, high alkalinity also occurs in pore solutions coming from deep-seated laumontite zones. This pore solution has a more complex chloride–sulfate sodium–

calcium composition, a high salinity (about 10 g/L), an increased silica concentration, and $\text{pH} = 8\text{--}10$ (Naboko, 1980). The lower characteristics of the pore solutions in the zone of shallow argillization of the EPF rocks are due to mixing of rising hydrothermal fluids with condensate water, as pointed out above, as well as to oxidation of sulfur-bearing compounds and iron salts in the solution (Sergeeva et al., 2022).

CONCLUSIONS

These studies have shown that zeolite mineralization occurs widely in the section of argillized rocks of the East Pauzhetka thermal field. The mineralization involves four zeolite types: laumontite, mordenite, heulandite-Ca, and stilbite-Ca. The latter is the most abundant.

Zeolites are formed in the zone of carbon dioxide leaching at relatively low pressures (between 2–3 and 6 atm) and temperatures below 150°C. The mineralizing solutions have characteristics similar to those of the hydrothermal fluids coming from the lower aquifer of the Pauzhetka geothermal field, namely, a chloride–sodium composition with a high concentration of carbonate ion and the dominance of alkaline-earth elements over alkaline elements, elevated concentra-

Table 4. Average (median) concentrations of components (g/L) in pore solutions found in contrasting zones of sulfuric acid leaching and carbon dioxide leaching in the EPF

Indicator, component	Sulfuric acid leaching zone, depth <3 m, $t < 70^{\circ}\text{C}$	Carbon dioxide leaching zone, depth >3 m, $t = 70-100-150^{\circ}\text{C}$
pH	3.69	7.09
HCO_3^-	0.001	0.589
F^-	0.003	0.01
Cl^-	0.028	0.071
SO_4^{2-}	1.686	0.311
Na^+	0.023	0.065
K^+	0.01	0.108
Ca^{2+}	0.017	0.39
Mg^{2+}	0.008	0.194
Fe^{2+}	0.028	0.005
Fe^{3+}	0.004	0.005
Al^{3+}	0.26	0.22
Sr^{2+}	0.00019	0.0006
Ba^{2+}	0.00024	0.00045
NH_4^+	0.008	0.022
H_3BO_3	0.007	0.014
H_4SiO_4 dissolv.	0.28	1.042
Salinity	2.3	2.4

The data on the concentrations of Al, Sr, and Ba were obtained using the method of inductively coupled plasma (ICP) at the Institute of Geochemistry, Siberian Branch RAS (Irkutsk) using a high resolution mass spectrometer for precision elemental analysis ICP/HRMS ELEMENT 2; the Analysts were G.P. Sandimirova and E.V. Smirnova. The other analyses were performed at the Analytical Center, IV&S FEB RAS (Petropavlovsk-Kamchatsky); the analysts were S.V. Sergeeva, V.V. Dunin-Barvovskaya, A.A. Kuzmina, and N.A. Solovieva.

tions of dissolved and colloidal silica and hydroxyaluminate ions, high concentrations of Sr and Ba, and pH = 6–8 (with ≥ 9 at the bottom of the section).

An analysis of a large data array for the chemical composition of each zeolite species (no such research has been done previously) showed that the composition of non-framework cations in zeolite minerals is controlled by the composition of thermal solutions enriched in elements that have been leached out of aluminosilicates; among these, the important members are elements such as Ca, Mg, Sr, Ba, Na, and K. The residence of these elements in zeolite structure seems to be primarily due to the structure of the zeolite itself and to its selectivity. As an example, the main concentrator of Ba and Sr among the zeolites during the later

phases of the hydrothermal process is the wide-pore heulandite-Ca with a sublayered framework structure. It is worth noting that Ba and Sr were determined for the first time in the zeolite minerals of the Puzhetka HS, and their presence in the zeolites furnishes another confirmation of the fact that the thermal solutions at depth are alkaline.

The spatial co-occurrence of different zeolite species in the EPF altered rocks shows that the zeolites are stable under these conditions. The species composition of the zeolites reflects changes in the physico-chemical parameters of the mineralizing environment, both in the hydrothermal system as a whole and in the shallow zone where hydrothermal fluids are discharged: one observes the general tendency of moderately siliceous laumontite in the propylites of the deeper horizons of the hydrothermal system and in the altered andesites of the bottom of the clay sequence giving way to high silica stilbite-Ca in the mudstones of the thermal field.

We thus see the confirmation of the general inference as to the regressive directivity for the hydrothermal alteration processes affecting the Puzhetka HS rocks, being seen as a successive change of phases of hydrothermal metamorphism from moderate-temperature propylites during the paleo phase to the present-day low-temperature mudstones (Korobov, 2019; *Struktura ...*, 1993). The rock temperature decreases from bottom to top along the section and the partial pressure of carbon dioxide decreases in the thermal waters rising toward the ground surface in a closed system, leaching them (increasing the alkalinity) and resulting in a wide occurrence of moderate-silica calcium zeolites, laumontite in the first place. In the shallow zone of argillization in an open system upon the background of all parameters of the mineralization environment decreasing, favorable conditions are created for deposition of mostly high silica calcium zeolites, largely from the stilbite group. The resulting sequence of zeolite generation (laumontite \rightarrow mordenite \rightarrow stilbite-Ca \rightarrow heulandite-Ca) in the zone of intensive discharge of alkaline solutions at the bottom of the hydrothermal clay sequence reflects, to a certain degree, the change of zeolite facies in the deeper horizons of the Puzhetka HS. This correlation is of great interest: the successive change of facies during zeolite generation in the shallow zone where hydrothermal fluids are discharged can furnish a criterion for assessing changes in the conditions of zeolite generation in the interior of a long-lived hydrothermal system.

ACKNOWLEDGMENTS

We are grateful to all colleagues at the South Kamchatka–Kuril Expedition for practical aid during field surveys and to personnel of the Analytical Center at the IV&S FEB RAS and the Institute of Geochemistry, Siberian Branch RAS (Irkutsk) for a large amount of analytical studies.

FUNDING

This work was supported by the Russian Foundation for Basic Research, project no. 19-05-00102.

REFERENCES

- Armbruster, T. and Gunter, M.E., Crystal structures of natural zeolites, *Rev. Mineral. Geochem.*, 2001, vol. 45, no. 1, pp. 1–67.
- Aoki, M., Hydrothermal alteration of chabazite, *J. Japan Assoc. Miner. Petr. Econom. Geol.*, 1978, vol. 73, pp. 155–166.
- Barth-Wirching, U. and Holler, H., Experimental studies on zeolite formation conditions, *Eur. J. Miner.*, 1989, vol. 1, no. 4, pp. 489–506.
- Belousov, V.I., Sugrobov, V.M., and Sugrobova, N.G., The geological structure and hydrogeological features of the Puzhetka hydrothermal system, in *Gidrotermal'nye sistemy i termal'nye polya Kamchatki* (The Geothermal Systems and Thermal Fields of Kamchatka), Vladivostok: DVNTs AN SSSR, 1976, pp. 23–57.
- Betekhtin, A.G., *Mineralogiya (Mineralogy)*, Moscow: Gosgeolizdat, 1950.
- Boles, J.R., Zeolites in deep-sea sediments. Mineralogy and geology of natural zeolites, *Miner. Soc. Amer.*, 1977, vol. 4, pp. 130–163.
- Burov, A.I., Kozovaya, T.V., Sibgatullin, A.Kh., et al., Zeolite-bearing rocks of Kamchatka, in *Prirodnye tseolity Rossii: geologiya, fiziko-khimicheskie svoystva i primeneniye v promyshlennosti i okhrane okruzhayushchei sredy* (Natural Zeolites of Russia: Geology, Physicochemical Properties, and Applications in Industries and Environment Protection), vol. 1, Novosibirsk: In-t Mineralogii i Petrografii SO RAN, 1992, pp. 45–48.
- Chelishchev, N.F., On the nomenclature and classification of naturally occurring zeolites, in *Prirodnye tseolity* (Natural Zeolites), Moscow: Nauka, 1980, pp. 99–103.
- Chelishchev, N.F., Bernshtein, B.G., and Volodin, V.F., *Tseolity—novyi tip mineralnogo syr'ya* (Zeolites—A New Type of Raw Minerals), Moscow: Nedra, 1987.
- Coombs, D.S., Alberti, A., Armbruster, T., et al., Recommended nomenclature for zeolite minerals: report of the subcommittee on zeolites of the international mineralogical association, commission on new minerals and mineral names, *The Canadian Mineralogist*, 1997, vol. 35, pp. 1571–1606.
- Coombs, D.S., Ellis, A.J., Fyfe, W.S., and Taylor, A.M., The zeolite facies with comments on the interpretation of hydrothermal syntheses, *Geochim. Cosmochim. Acta*, 1959, vol. 17, nos. 1/2, pp. 53–107.
- Distanov, U.G., Mikhailov, A.S., Konyukhova, T.P., et al., *Prirodnye sorbenty SSSR* (Naturally Occurring Sorbents in the USSR), Moscow: Nedra, 1990.
- Dolgozhivushchii tsentr endogennoi aktivnosti vulkanov yuzhnoi Kamchatki (The Long-Lived Center of Endogenous Activity of Southern Kamchatka Volcanoes), Masurenkov, Yu.P., Editor-in-Chief, Moscow: Nauka, 1980.
- Eroshchev-Shak, V.A., *Gidrotermal'nyi subpoverkhnostnyi litogenez Kurilo-Kamchatskogo regiona* (The Hydrothermal Subsurface Lithogenesis in the Kuril–Kamchatka Region), Moscow: Nauka, 1992.
- Feofilaktov, S.O., Rychagov, S.N., Bukatov, Yu.Yu., Nuzhdaev, I.A., and Nuzhdaev, A.A., New evidence relating to the structure of the zone of hydrothermal discharges in the East Puzhetka Thermal Field, Kamchatka, *J. Volcanol. Seismol.*, 2017, vol. 11, no. 5, pp. 353–366.
- Fersman, A.E., *Tseolity Rossii i ikh mineralogiya* (Russian Zeolites and Their Mineralogy), Moscow: AN SSSR, 1952, pp. 567–702.
- Godovikov, A.A., *Mineralogiya (Mineralogy)*, Moscow: Nedra, 1975.
- Gottardi, G., The genesis of zeolites, *Eur. J. Mineral.*, 1989, vol. 1, no. 4, pp. 479–487.
- Gottardi, G. and Galli, E., *Natural Zeolites*, Part of the Minerals and Rocks book series Minerals, 1985, vol. 18.
- Iler, R., *The Chemistry of Silica: Solubility, Polymerization, Colloid and Surface Properties and Biochemistry of Silica*, Wiley, 1979.
- Jijima, A. and Utada, M., A critical review on the occurrence of zeolites in sedimentary rocks in Japan, *Jap. J. Geol. Geogr.*, 1972, vol. 42, nos. 1/4, pp. 61–83.
- Karpov, G.A., *Eksperimentalnoe mineraloobrazovanie v geotermalnykh skvazhinakh* (Experimental Mineral Generation in Geothermal Wells), Moscow: Nauka, 1976.
- Koporulin, V.I., On the generation of laumontite in sedimentary deposits: Sedimentary sequences in Russia, *Litol. Polezn. Iskop.*, 2013, no. 2, pp. 128–144.
- Korobov, A.D., *Gidrotermalniy litogenez v oblastiakh nazemnogo vulkanizma* (Hydrothermal Lithogeny in Areas of Land Volcanism), Saratov: Saratovskii Un-t, 2019.
- Korobov, A.D., Goncharenko, O.P., Rikhter, Ya.A., et al., The phases of postmagmatic processes in the Puzhetka hydrothermal system, southern Kamchatka, in *Sovremennoe vulkanogenno-gidrotermalnoe mineraloobrazovanie* (Present-Day Hydrothermal Mineral Generation and Mineralization), Part I, Vladivostok, 1992, pp. 81–94.
- Kossovskaya, A.G., Genetic types of zeolites in stratified formations, *Litol. Polezn. Iskop.*, 1975, no. 2, pp. 23–44.
- Kossovskaya, A.G., Shutov, V.D., and Kats, M.Ya., Genetic types of zeolites in the Clinoptilolite-heulandite group of continents and oceans, in *Prirodnye Tseolity* (Naturally Occurring Zeolites), Moscow: Nauka, 1980, pp. 8–30.
- Lazarenko, E.K., *Kurs mineralogii* (A Course in Mineralogy), Moscow: Vysshaya Shkola, 1971.
- Lebedev, L.M., *Mineraly sovremennykh gidroterm* (Minerals in Present-Day Hydrothermal Discharges), Moscow: Nauka, 1979.
- Liou, J.G., Stilbite–laumontite equilibrium, *Contrib. Miner. Petrol.*, 1971, vol. 31, no. 3, pp. 171–177.
- Mamedova, G.A., The modification of naturally occurring zeolite in Nakhchivan in an alkaline environment, *Vestn. Moscow University, Ser. 2, Chemistry*, 2019, vol. 60, no. 1, pp. 65–73.
- Marantos, I., Christidis, G.E., and Ulmanu, M., Zeolite formation and deposits, in *Natural Zeolites Handbook*, Bentham Science Publishers Ltd, 2011, pp. 19–36.

- The Encyclopedia of Mineralogy*, Frye, K., Ed., 1981, Springer Science and Business Media.
- Moncure, G.K., Surdam, R.C., and Mokague, H.L., Zeolite diagenesis below Pahute Mesa, Nevada test site, *Clays and Clay Miner.*, 1981, vol. 29, no. 5, pp. 385–396.
- Mumpton, F.A., La roca magica: Uses of natural zeolites in agriculture and industry, *Proc. Nat. Acad. Sci. United States of America J.*, 1999, vol. 96, no. 7, pp. 3463–3470.
- Naboko, S.I., *Gidrotermalniy metamorfizm porod v vulkanicheskikh oblastiakh* (Hydrothermal Metamorphism of Rocks in Volcanic Areas), Moscow: AN SSSR, 1963.
- Naboko, S.I., Patterns in the generation of zeolite rocks in areas of hydrothermal discharges, in *Prirodnye tseolity* (Natural Zeolites), Moscow: Nauka, 1980, pp. 38–53.
- Naboko, S.I. and Glavatskikh, S.F., High silica zeolites in the Geyser Valley, Kamchatka, *Byull. Vulkanol. St.*, 1978, no. 55, pp. 101–106.
- Naboko, S.I., Karpov, G.A., and Roznikova, A.P., Hydrothermal metamorphism of rocks and mineralization, in *Pauzhetskie goryachie vody na Kamchatke* (Pauzhetka Hot Waters in Kamchatka), Moscow: Nauka, 1965, pp. 76–118.
- Naboko, S.I. and Lebedev, L.M., Present-day generation of laumontite in Pauzhetka, in *Sovremenniy vulkanizm Severo-Vostochnoi Sibiri* (The Present-Day Volcanism of northeastern Siberia), Moscow: Nauka, 1964, pp. 78–83.
- Nasedkin, V.V., Solovieva, T.N., Nistratova, I.E., et al., Comparative characterization of the mineral composition of zeolite rocks on Mt. Yagodnaya and of products of present-day volcanism in the Bannaya River valley, Kamchatka, in *Sovremennye gidrotermny i mineraloobrazovanie* (Present-Day Hydrothermal Discharges and Mineral Generation), Moscow: Nauka, 1988, pp. 70–85.
- Ortiz, F.A.Q., Valenzuela, J.T., and Reyes, C.A.R., Zeolitization of Neogene sedimentary and pyroclastic rocks exposed in Paipa (Boyaca), in the Colombian Andes: simulating their natural formation conditions, *Earth Sci. Res. J.*, 2011, vol. 15, no. 2, pp. 2–20.
- Pampura, V.D., *Mineraloobrazovanie v gidrotermalnykh sistemakh* (Mineral Generation in Hydrothermal Systems), Moscow: Nauka, 1977.
- Pampura, V.D., Hydrothermal activity in the Pauzhetka volcano-tectonic depression, in *Dolgozhivushchii tsentr endogennoi aktivnosti vulkanov yuzhnoi Kamchatki* (The Long-Lived Center of Endogenous Activity of Southern Kamchatka Volcanoes), Masurenkov, Yu.P., Editor-in-Chief, Moscow: Nauka, 1980, pp. 139–156.
- Passaglia, E. and Sheppard, R.A., *The crystal chemistry of zeolites, Natural Zeolites: Occurrence, Properties, Applications*. Reviews in Mineralogy and Geochemistry, 2001, vol. 45, pp. 69–116.
- Passaglia, E., The crystal chemistry of chabazites, *American Mineralogist*, 1970, vol. 55, pp. 1278–1301.
- Pauzhetskie goryachie vody na Kamchatke* (The Pauzhetka Hot Waters in Kamchatka), Moscow: Nauka, 1965.
- Pekov, I.V., Turchkova, A.G., Lovskaya, E.V., et al., *Tseolity shchelochnykh massivov* (Zeolites in Alkaline Massifs), Moscow: Ekost, 2004.
- Petrova, V.V., *Nizkotemperaturnye vtorichnye mineraly i ikh rol v litogeneze* (Low Temperature Secondary Minerals and Their Role in Lithogeny), Moscow: GEOS, 2005.
- Prirodnye tseolity* (Natural Zeolites), Kossovskaya, A.G., Ed., Moscow: Nauka, 1980.
- Rochler, H.W., Zonal distribution of montmorillonite and zeolites in Laney Shala Member of the Green River Formation in the Washakie Basin, Wyoming, *Geol. Survey Professional Paper*, Washington: United States Government Printing Office, 1972, no. 800-B, pp. 121–124.
- Rychagov, S.N., Davletbaev, R.G., and Kovina, O.V., Hydrothermal clays and pyrite in geothermal fields: Their significance for the geochemistry of present-day endogenous processes in southern Kamchatka, *J. Volcanol. Seismol.*, 2009, vol. 3, no. 2, pp. 105–120.
- Rychagov, S.N., Sergeeva, A.V., and Chernov, M.S., Mineral associations at the base of a clay mass as indicators of fluid regime in the Pauzhetka Hydrothermal System, Kamchatka, *Tikhookean. Geol.*, 2017, vol. 36, no. 6, pp. 90–106.
- Rychagov, S.N., Sandimirova, E.I., Chernov, M.S., and Sergeeva, A.V., Formation of alkaline mineralization in acid leaching zone of Pauzhetka Hydrothermal System (South Kamchatka), *Proc. XXXV International Conference, Magmatism of the Earth and Related Strategic Metal Deposits*, Moscow, 3–7 September 2018, Moscow: GEOKHI RAS, 2018, pp. 255–259.
- Rychagov, S.N., Kravchenko, O.V., Nuzhdaev, A.A., and Chernov, M.S., The lithology of the clay sequence in the East Pauzhetka thermal field, southern Kamchatka, in *Materialy XXII nauchnoi konferentsii, posvyashchennoi Dnyu vulkanologa “Vulkanizm i svyazannye s nim protsessy* (Proc. XXII Conf. Devoted to Volcanologist’s Day, Volcanism and Related Processes), March 28–29, 2019, Petropavlovsk-Kamchatsky: IViS DVO RAN, 2019, pp. 213–216.
- Rychagov, S.N., Sandimirova, E.I., Kravchenko, O.V., and Chernov, M.S., The influence of alkaline fluids on the argillization zone of a present-day hydrothermal system, in *Materialy XIII Vserossiiskogo Petrograficheskogo soveshchaniya (s uchastien zarubezhnykh uchenykh) “Petrogiya i geodinamika geologicheskikh protsessov”* (Proc. XIII All-Russia Petrographic Conference (with participation of scientists from abroad) “Petrography and Geodynamics of Geological Processes”), Irkutsk, September 6–13, 2021, Irkutsk: Institut Geografii im. V.B. Sochavy SO RAN, 2021, vol. 3, pp. 25–29.
- Sandimirova, E.I., Rychagov, S.N., and Chubarov, V.M., Zeolites in mudstones of the East Pauzhetka thermal field, southern Kamchatka, in *Materialy XIII Vserossiiskogo Petrograficheskogo soveshchaniya (s uchastien zarubezhnykh uchenykh) “Petrogiya i geodinamika geologicheskikh protsessov”* (Proc. XIII All-Russia Petrographic Conference (with participation of scientists from abroad) “Petrography and Geodynamics of Geological Processes”), Irkutsk, September 6–13, 2021, Irkutsk: Institut Geografii im. V.B. Sochavy SO RAN, 2021, vol. 3, pp. 52–54.
- Senderov, E.E. and Khitarov, N.I., *Tseolity, ikh sintez i usloviya obrazovaniya v prirode* (Zeolites, Their Synthesis, and the Conditions of Generation in Nature), Moscow: Nauka, 1970.

- Sergeeva, A.V., A spectral characteristic of laumontite sampled in the East Pauzhetka thermal field, in in *Materialy XXII nauchnoi konferentsii, posvyashchennoi Dnyu vulkanologa "Vulkanizm i svyazannye s nim protsessy"* (Proc. XXII Conf. Devoted to Volcanologist's Day, Volcanism and Related Processes), March 28–29, 2019, Petropavlovsk-Kamchatsky: IViS DVO RAN, 2019, pp. 228–231.
- Sergeeva, A.V., Zhitova, E.S., Nuzhdaev, A.A., and Nazarova, M.A., Modeling the process of mineral generation in thermal anomalies with ammonium sulfate thermal waters: The role of pH, *J. Volcanol. Seismol.*, 2022, vol. 16, no. 1, pp. 35–48.
- Sheppard, R.A., Zeolites in sedimentary rocks, *Geol. Survey Professional Paper*, Washington: United States Government Printing Office, 1973, no. 820, pp. 279–310.
- Sheppard, R.A. and Gude, A.J., Zeolites and Associated Authigenic Silicate Minerals in Tuffaceous Rocks of the Big Sandy Formation, Mohave County, Arizona, *Geol. Survey Professional Paper*, Washington: United States Government Printing Office, 1973, no. 830, pp. 543–578.
- Seryotkin, Y.V., Influence of content of pressure-transmitting medium on structural evolution of heulandite: Single-crystal X-ray diffraction study, *Microporous and Mesoporous Materials*, 2015, vol. 214, pp. 127–135.
- Shevchuk, V.D., Perspectives and problems in the industrial applications of naturally occurring zeolites of Kamchatka, *Gornyi Vestn. Kamch.*, 2008, no. 3, pp. 32–34.
- Smith, J.V., Rinaldi, R., and Dent Glasser, L.S., Structures with a chabazite framework: II. Hydrated Ca-chabazite at room temperature, *Acta Crystallogr.*, 1963, vol. 16, pp. 45–53.
- Struktura gidrotermalnoi sistemy (The Structure of the Hydrothermal System)*, Moscow: Nauka, 1993.
- Suprychev, V.A., Zeolites of volcanogenic and plutogenic ore formations, *Izv. Vuzov, Geol. Razv.*, 1978, no. 9, pp. 54–60.
- Suprychev, V.A., Metagenetic zeolites of catagenesis and protometamorphism phases in sedimentary and sedimentary-volcanogenic formations, *Izv. Vuzov, Geol. Razv.*, 1980, no. 1, pp. 37–42.
- Suprychev, V.A. and Kirikilitza, S.I., *Geneticheskaya tipizatsiya tseolotov stratifitsirovannykh formatsii* (A Genetic Classification of Zeolites in Stratified Formations), Moscow: Nauka, 1980.
- Zhdanov, S.P., Khvoshchev, S.S., and Samulevich, N.N., *Sinteticheskie tseolity: kristallizatsiya, strukturno-khimicheskoe modifitsirovanie, adsorbtsionnye svoistva* (Synthetic Zeolites: Crystallization, Structural Chemical Modification, Adsorption), Moscow: Khimiya, 1981.
- Zozulya, D.R., Kullerud, K., Ravna, E.K., et al., Mineralogical and geochemical constraints on magma evolution and late-stage crystallization history of the Breivikboth silicocarbonatite, Seiland Igneous Province in northern Norway: Prerequisites for zeolite deposits in carbonatite complexes, *Minerals*, 2018, vol. 8, no. 537, pp. 1–23.

Translated by A. Petrosyan